Tutor/s

Dr. Rodrigo Soto Lopez
Departament de catàlisi i cinètica aplicada
Dr. Roger Bringué Tomàs
Departament de catàlisi i cinètica aplicada

Grau en Enginyeria Química

Treball Final de Grau

Synthesis of mesityl oxide from acetone using acidic ion-exchange resins as catalysts

Mònica Rodríguez Sayrol

June 2022

UNIVERSITAT DE BARCELONA

Una persona que mai va cometre un error, mai va intentar alguna cosa nova.

Albert Einstein

En primer lloc, m'agradaria agrair als meus tutors, Dr Rodrigo Soto i Dr. Roger Bringué. Gràcies per l'oportunitat de poder treballar amb vosaltres, per la paciència, la confiança i l'ajuda que se m'ha proporcionat durant aquests últims mesos. Gràcies de nou Rodrigo, per estar present en cada experiment realitzat i per anar guiant-nos en cada pas.

Seguidament, vull agrair a tots els meus amics per fer-me sentir tan afortunada, estimada i haver sigut un suport incondicional.

Per últim, agrair a la meva família, en especial a la meva germana, la meva mare i el meu pare. Per ser el meu pilar fonamental, per tots els consells i ànims, i perquè tot el que he aconseguit és en gran part gràcies a ells.

CONTENTS

SUMMARY

Acetone, one of the most widely used organic solvents, is mainly synthesized from crude oil. However, in recent decades, other more sustainable production processes have been gaining importance. Acetone, in addition to being able to be produced via biosynthetic routes, can be a starting chemical for synthesizing a range of solvents of chemical interest. One of the solvents produced from acetone is mesityl oxide, formed through a two-reaction in series system via acid catalysis, for example by ion exchange resins. As they are solid catalysts, the separation of the final product is a straightforward process. However, they can present transfer limitations through the phases and limit the reaction, therefore, the accessibility to the active centres of the catalysts plays a fundamental role in the progress of a reaction. The catalytic activity will depend on the catalyst morphological properties and the nature of the active sites. In the present project, the liquid-phase synthesis of mesityl oxide is studied over a wide array of macroporous ion exchange resins. The main aim is to identify the catalyst properties that favor the formation of mesityl oxide.

From the experiments performed, the results obtained at he explored conditions indicated high selectivity for all the catalysts used and noteworthy, by-products were not detected in any of the runs performed excepting for the mesityl oxide isomer, which was obtained in very low amount. The acetone conversions ranged 3-15%. The experimental initial formation rates of mesityl oxide are estimated and related to the properties of the resins studied. As a main conclusion, high acid capacity was found to be the most relevant property, combined with a low ability to swell in the reaction medium, promoting eventually the synthesis of mesityl oxide. Among the catalysts studied, the best resin in terms of conversion, selectivity and conversion formation rates is A-35.

Keywords: Mesityl oxide, ion exchange resins, macroreticular, swelling, catalytic activity.

.

RESUM

L'acetona, un dels dissolvents orgànics més utilitzats, es sintetitza principalment a partir del petroli cru. Tanmateix, en les últimes dècades, altres processos de producció més sostenibles han anat guanyant importància. L'acetona, a més de poder produir-se per vies biosintètiques, pot ser un producte químic de partida per sintetitzar una sèrie de dissolvents d'interès químic. Un dels dissolvents produïts a partir de l'acetona és l'òxid de mesitil, format mitjançant un sistema de dues reaccions en sèrie per catàlisi àcida, per exemple amb resines d'intercanvi iònic. Com que són catalitzadors sòlids, la separació del producte final és un procés senzill. Tanmateix, poden presentar limitacions de transferència a través de les fases i limitar la reacció, per tant, l'accessibilitat als centres actius dels catalitzadors juga un paper fonamental en el progrés d'una reacció. L'activitat catalítica dependrà de les propietats morfològiques del catalitzador i de la naturalesa dels llocs actius. En el present projecte, s'estudia la síntesi en fase líquida d'òxid de mesitil sobre una àmplia gamma de resines d'intercanvi iònic macroporoses. L'objectiu principal és identificar les propietats del catalitzador que afavoreixen la formació d'òxid de mesitil.

A partir dels experiments realitzats, en les condicions explorades els resultats van indicar una alta selectivitat per a tots els catalitzadors utilitzats i cal destacar que no es van detectar subproductes en cap de les tirades realitzades excepte l'isòmer de l'òxid de mesitil, que es va obtenir en quantitat molt baixa. Les conversions d'acetona van oscil·lar entre el 3 i el 15%. S'estimen les taxes experimentals de formació inicial d'òxid de mesitil i es relacionen amb les propietats de les resines estudiades. Com a conclusió principal, es va trobar que l'alta capacitat àcida era la propietat més rellevant, combinada amb una baixa capacitat d'inflar-se en el medi de reacció, afavorint finalment la síntesi d'òxid de mesitil. Entre els catalitzadors estudiats, la millor resina en termes de conversió, selectivitat i velocitats de formació de conversió és l'A-35.

Paraules clau: Òxid de mesitil, resines d'intercanvi iònic, macroreticular, inflor, activitat catalítica.

1. INTRODUCTION

A solvent is a chemical substance in which a solute is dissolved, resulting in a solution. The solvent is often the major component of a formulation step, e.g. the chemical reaction or the extraction process. Solvents have various applications that are essential for many products to act effectively as components in paints, pharmaceuticals, adhesives, production of synthetic materials, among others, as it can be seen in *Figure 1*. Today the most common solvents are organic, which are used to dissolve raw material, products or waste, as a cleaning agent, dispersing agent, surfactant or density modifier [1]. The present day solvent market is on the order of 20 million metric tonnes (MMT) and worth tens of billions of US dollars annually to the global economy [2].

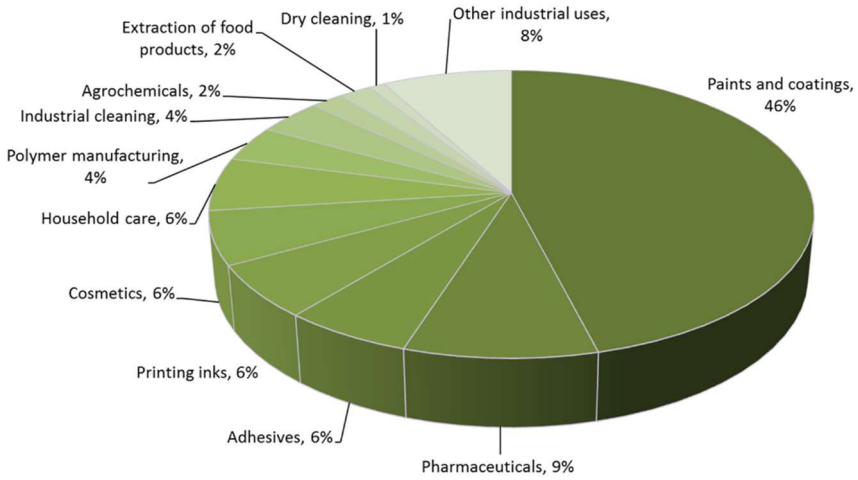

Figure 1. Solvent use arranged by sector [2]

Most solvents are manufactured from crude oil. The manufacturing process is highly integrated into the operation of a petroleum refinery or petrochemical manufacturing plant. One of the most popular solvents that comes from petroleum is acetone. On its most common production process, benzene reacts with propylene to form cumene, which is subsequently oxidized to form cumene hydroperoxide. Then, in the presence of sulfuric acid, it finally forms phenol and acetone. From each tone of phenol, 0.62 tons of acetone are formed. In 2020, the market volume of acetone worldwide amounted to nearly 6.7 million tons [3]. Although nearly 90% of acetone is produced by cumene process, it can also be synthesized using other chemical routes based on renewable feedstocks. Considering that the accelerating climate crisis requires environmentally sustainable and carbon-negative processes, nowadays the main objective in future processes is to replace fossil-fuel product formation with sustainable alternatives [4].

Only about 10% of solvents are manufactured using other feedstocks (natural gas, coal or biomass) [5]. In recent decades, solvents obtained by different routes, such as from biomass or biosynthetics, have gained prominence. Acetone could be made more sustainably through the well-known ABE fermentation process. Acetone-butanol-ethanol (ABE) fermentation is a biocatalytic process that uses a microorganism to process carbohydrates (fructose, sucrose, glucose, etc.) to generate solvent end products. One of the microorganisms used to generate acetone, butanol and ethanol from various carbon sources such as glucose, galactose, cellobiose, mannose, xylose and arabinose is *Clostridium* [6].

Consequently, acetone is a type of organic solvent which, in addition to being able to be produced on a large scale by a biosynthetic process, can give rise to a new range of solvents. One of the most valuable acetone solvent derivate is methyl isobutyl ketone (MIBK). It is used primarily as a solvent in the paint and coating industries, metallurgical extraction, and pharmaceutical manufacturing processes. It is also used as a precursor in the synthesis of speciality chemicals including pesticides, surfactants, and rubber antioxidants as well as a flavouring agent and in food-contact packaging products [7]. The current global demand of MIBK exceeds 300 kton/year, with an expected Compound Annual Growth Rate of 7.5 % over the period 2016–2024 [8].

The precursor for the syntesis of MIBK by metal-catalysed selective hydrogenation is mesityl oxide (MSO), which is produced from the MIBK synthesis process starting from acetone. This compound is a colourless, volatile, and flammable liquid at room conditions and presents certain

toxicity. It is a trifunctional intermediate of great utility in the synthesis of different types of organic compounds, pharmaceutical chemistry, polymer, and material science.

1.1. METHYL ISOBUTYL KETONE FROM ACETONE

The reaction to obtain MIBK requires three consecutive steps, as illustrated in *Figure 2*. First, diacetone alcohol (DAA) is formed by acid or base-mediated aldol condensation of acetone, which is subsequently dehydrated in presence of an acid catalyst, forming thereby MSO. Finally, by metal-catalysed selective hydrogenation, MIBK is formed by saturating the carbon double bond functional group of MSO.

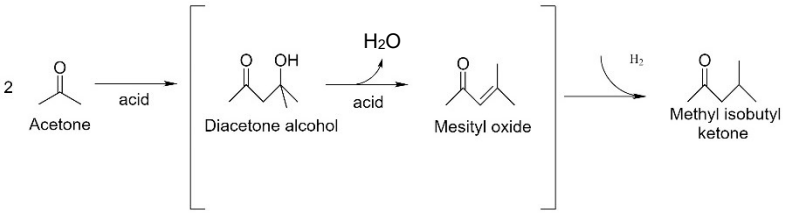

Figure 2. Reaction pathway for the synthesis of methyl isobutyl ketone from acetone.

1.1.1. The three consecutive reaction steps

The formation of diacetone alcohol from acetone is an aldol condensation. Generally, the aldol condensation of aldehydes and ketones is used in organic synthesis processes to produce chemicals containing a conjugated double bond with the carbonyl group [9].

In aldol condensation, a carbanion reacts with the carbonyl group of a second acetone molecule and after catalytic deprotonation the diacetone alcohol is formed. This is a catalytic reaction, usually in a basic medium, where the reaction products are α-β-unsaturated carbonyls. However, it could also occur in an acidic medium, yielding hydrocarbons. Then, the catalyst removes H^+ from the hydroxyl group of the alcohol to form an aldol anion. The following step is the scission of the carbon-carbon bond in the aldol with the formation of acetone and the acetone carbanion. The reaction terminates with the addition of the proton to the carbanion resulting in a second molecule of the reaction product plus acetone [10]. Nevertheless, in the presence of acids,

the catalysed reaction rapidly dehydrates to give α-β-unsaturated ketone, mesityl oxide. It is a highly reversible reaction where the water absorbed by the catalyst can hydrate the mesityl oxide to form acetone. For this reason, the absence of water is required to stabilise mesityl oxide. If the objective of the process is the production of methyl isobutyl ketone, which ultimately occurs in the process is the selective liquid phase hydrogenation of unsaturated MSO to form MIBK, therefore maximizing the MSO production becomes crucial towards the optimization of the MIBK production process.

1.1.2. Formation process

The conventional MIBK production process consisted in using multiple reactors and processing units in each step of the reaction. However, this process generates a huge amount of waste, and it is economically and technically unfavourable. Thanks to the use of heterogeneous bifunctional catalysts with combined acid-base and hydrogenation properties, the reaction of acetone to produce MSO and subsequently MIBK occurs by consecutively combining condensation, subsequent dehydration and finally hydrogenation of the reaction in a single step [8].

The most studied bifunctional catalysts are those loaded with different metals of the Periodic Table such as palladium (Pd), copper (Cu) and platinum (Pt) on acidic supports. There are different types of acid/base catalytic supports such as aluminosilicates, zeolites, metal oxides and ion exchange resins. The ion exchange resin can be loaded with the desired metal ions, usually in the form of metal salts, such as chlorides, bromides, nitrates, sulphates and acetates [11].

This combined synthesis has been studied in liquid and gas phase. Liquid phase studies have been carried out at pressures ranging from 10 to 100 bar and temperatures from 120 to 160 ^{o}C using palladium on different acid-base supports and a cation exchange resin. In these studies, hydrogen gas was dissolved in the reaction mixture. Acetone conversions ranging from 30-50% were obtained with high MIBK (>90%). Gas phase studies were performed at atmospheric pressure, although reaction temperatures similar to liquid phase reactions are used. Different metals were used on different acid-base supports. Most of the gas phase studies have lower MIBK selectivities (<80%) as catalyst deactivation appears to be more severe for the gas phase reaction [11].

However, under the concurrent conditions of acidic and hydrogenation catalysis, synthesis of MIBK from acetone may undergo a very complex set of reactions, resulting in a variety of C3, C6, C9 and C12 by-products, due to the simultaneous possible condensation, dehydration, isomerisation and hydrogenation side-reactions. This reaction has numerous by-products as it can be seen in *Figure 3*. The most common ones are isophorone, mesitylene and phorone, which are also important organic compounds in the chemical industry.

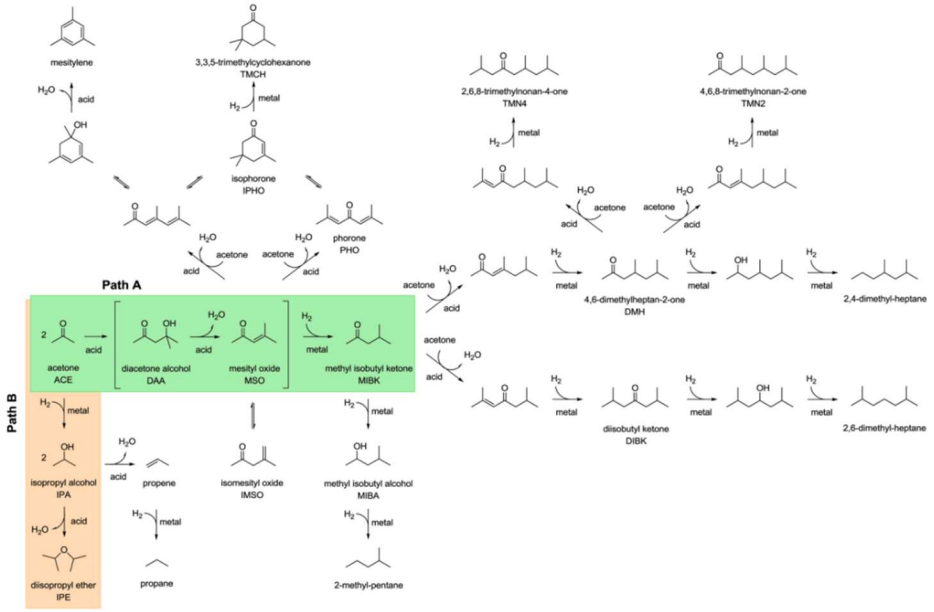

Figure 3. Possible reactions in the synthesis of MIBK from acetone via dehydration of MSO [21]

1.1.3. State of art

Acetone, an easily available chemical, has numerous by-products of great interest. MIBK is one of its most prized derivatives, so there is a lot of literature on its three reaction steps of formation from acetone.

In recent studies [12], one-step synthesis of methyl isobutyl ketone from acetone and hydrogen using Amberlyst®CH28, a commercial palladium impregnated cation exchange resin catalyst, in a lab scale trickle bed reactor. The study found that dehydration of DAA to give MSO limited the productivity of the catalyst, a fact attributed to the water formed from the reaction.

The solvent-free hydrogenation reaction of acetone synthesizing methyl isobutyl ketone over bifunctional heterogeneous catalysts [8], comprising cross-linked perfluorosulfonic acid (PFSA) resins and supported Pd nanoparticles, was investigated in liquid phase under batch conditions. The best compromise results between selectivity and productivity were obtained for a catalyst that is based on 0.8 % cross-linked PFSA support and 0.26 wt.% Pd content.

Other studies focused on the use of catalytic distillation (CD) technology [7] to synthesize MSO and MIBK from acetone, comparing with commercial reference catalysts. By using CD technology, undesired consecutive reactions can be minimized, and, at the same time, the production of a desired intermediate species can be increased. However, the yield of MIBK was relatively low, mainly due to the deactivation of the hydrogenation catalyst and aggravated by the relatively low system pressures used in the hydrogenation experiments.

The reaction system has also been used to study the properties of catalysts. As an example, the decomposition of diacetone alcohol can be considered as test reactions useful for investigating the basic properties of solid catalysts [10].

However, there is not much literature to encourage the production of MSO, formed in the second step of the reaction. An increase of the formation of this product could consequently benefit the formation of MIBK. A screening will be performed with different macroporous ion exchange resins with different properties to determine which characteristics favour the formation of MSO.

1.2. **CATALYST**

The main function of a catalyst is to decrease the activation energy of a chemical process. The use of catalytic materials plays a fundamental role in the production of many chemical products in the global industry [13]. It is estimated that 50% of current industrial chemical production processes are based on catalytic reactions. Among them, heterogeneous catalysis represents the 80%. Considering the phase in which the catalyst and the reactants are, catalysts are classified as homogenous or heterogenous. Homogenous catalysts are on the same phase

of one of the reactants and their selectivity is high. However, they have disadvantages in terms of experimental conditions such as temperature and pressure, and primarily problems in their separation from the reacting mixture, as well as the fact that they can be toxic and damage working equipment. On the other hand, there are heterogeneous catalysts, which are not in the same phase as the reactants. The catalyst is usually in the solid phase. This makes it easier to separate the catalyst from the final product. Their main advantages are to prevent the corrosion of the different parts of the industrial plants, ease for separating products, less pollution potential of waste streams, easy for recycling and reaction rates and that often the process selectivity is higher. Despite these advantages, using a solid catalyst can affect the evolution of the reaction as it includes the limitation of transfer between phases, conditioning the accessibility of the reactants to the active centres.

For a solid to act as a catalyst, at least one of the reactants must interact with its surface to be adsorbed. Therefore, having a large surface area is an essential structural property. Porous solids are known to feature a large surface area per mass unit. The structure of solid catalyst particles (number, size, and pore volume) is elemental for the catalyst to operate properly. Reactant adsorption, reaction and desorption are the different chemical stages of a solid catalyst particle that take place on the catalyst surface, named active centre. The type of adsorption is specific for each catalyst depending on the type of catalytic reaction performed [14].

1.2.1. Ion-exchange resins

Ion-exchange resins (IER) are solid organic materials composed by a skeleton or polymeric matrix formed by hydrocarbon chains joined together that constitutes a tridimensional structure of hydrophobic nature in which functional groups, normally of hydrophilic nature, are anchored. Ion-exchange resins are useful because of the insolubility of the resin phase. After contact with the ion-containing solution, the resin can be separated by filtration. They are also adaptable to continuous processes involving columns and chromatographic separations. Their insolubility renders them environmentally compatible since the cycle of loading, regeneration and reloading allows them to be used for many years. Ion-exchange resins have been used in water softening, removal of toxic metals from water in the environment, wastewater treatment, hydrometallurgy, sensors, chromatography, and biomolecular separations [15]. They have also been widely used

as catalysts, in manifold chemical reactions such as oligomerization of olefins etherification of alcohols with olefins, esterification of fatty acids with alcohols, dehydration of alcohols among others [13].

One of the most common types of ion-exchange resins are polystyrene-divinylbenze (PS-DVB) resins. PS-DVB resins are synthesized by the suspension or copolymerization of styrene (addition) and dinivylbenzene. Styrene polymerization in the presence of at least a small amount (1%) of a divinylic compound, as 1,4-divinylbenzene (DVB) creates a cross-linked polymer insoluble in common organic solvents. Though the crosslinking is a complex phenomenon, DVB typically acts as crosslinker between two linear chains of polystyrene. The mechanism of copolymerization by addition shown in *Figure 4*, also called vinyl polymerization, is a free radical induced polymerization between reactants (monomers) carrying ethenyl (or vinyl) double bonds (-CH=CH_2). One of the reactants must contain at least two ethenyl double bonds to effect crosslinking. The extent to which the copolymer is crosslinked depends upon the proportion of crosslinking agent (DVB) used in the synthesis and has a pronounced impact upon both the mechanical and chemical behavior of the derived ion-exchange resin. Correct reaction conditions and the use of suspension stabilizers enable the control of the particle size distribution. Functionalization (activation) of such supports provides catalytic activity to the resins [13].

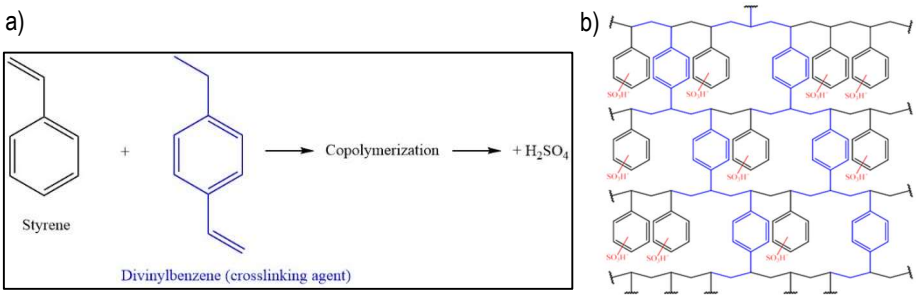

Figure 4. a) Synthesis of polystyrene-divinylbenze (PS-DVB) resins. b) Example of the structure of polystyrene-divinylbenze (PS-DVB) resins.

1.2.1.1. Properties of styrene divinylbenzene resins

The effectiveness of a catalyst given a reaction depends on its properties. The properties of a resin are determined by the nature of the monomer, the method of polymerisation, the degree of crosslinking and the nature of the functional groups anchored to the polymer matrix. The catalytic activity is influenced by the properties of the resin such as the acid or basic strength, the structure, active sites concentration and their accessibility, the structure of pores and distribution, the degree of swelling (fundamental to control substrate accessibility), and the ease of diffusion of involved species [13]. The most relevant properties of IER and how they can be determined are explained below:

- **Functionalization degree.** It represents the percentage of aromatic rings that have been functionalized.

- **Ion-exchange capacity.** It is expressed as the number of functional groups that the resin can introduce in ion exchange reactions. It is usually measured as milliequivalents of functional group per dry gram of resin, e.g. meqH+/g for sulphonic IER.

- **Crosslinking degree.** It represents the percentage by weight of the crosslinking agent in relation to the total weight of the monomers before the copolymerization takes place. It is usually expressed as "%DVB".

- **Porosity (θ).** The intrinsic porosity of an IER refers to the hollows that remain between the polymer chains that form the matrix

- **Surface or specific area (S_g).** It is the total surface area of the particle (external and pores) per gram of dry solid.

- **Pore Volume (V_g) and pore distribution**. It is defined as the volume of pores per gram of dry solid. Depending on the pore size or pore diameter (dpore) the following pore distribution can be distinguished: micro (<2nm), meso (2nm<dpore<50nm) or macropores (>50nm).

- **Stability**. Resins stability is a property of utmost importance since as catalyst they must remain operative for long lasting periods. IER must show chemical, thermal and mechanical stability.

- **Density or skeletal density (ρs).** It is defined as the weight of dry resin per unit of volume of solid.

- **Moisture content.** It is defined as the ratio of the weight of water within the resin to the total weight of hydrated resin. IER contain some water linked to the structure due to the hydrophilic nature of the active sites.

- **Swelling degree.** IER are known to swell, being the swelling more pronounced in polar solvents as water or alcohols. Several factors are involved in the swelling phenomenon as the temperature, the chemical nature of the solvent (polar or non-polar), the resin crosslinking degree, the nature of the functional groups and its concentration. It is an important attribute of a resins as the catalytic activity of ion exchange depends on their swelling properties and it is a fundamental property to be considered for loading industrial reactors. The resin swells, because of a portion of the liquid component is absorbed by the resin up to reaching equilibrium with the liquid phase [15].

1.2.2. Acidic ion exchange resins

Depending on the foreseen application, functional groups can be acid, basic, redox or even metallic complexes. Ion exchange resins that are classified as cation exchangers, having positively charged mobile ions available for exchange, and those whose exchangeable ions are negatively charged, the so-called anion exchangers. Both anion and cation resins are produced from the same basic organic polymers. They differ in the ionizable group attached to the hydrocarbon network. It is this functional group that determines the chemical behaviour of the resin. Resins can be broadly classified as strong or weak acid cation exchangers or strong or weak base anion exchangers [17].

While basic resins present some limitations for industrial application, primarily because of their low stability at temperature above 50 ^{o}C, acid resins are well established catalysts in the large-scale manufacture of chemicals. For instance, these resins are employed to produce methyl isobutyl ketone (MIBK) from acetone, isopropyl alcohol (IPA) by propylene hydration and mainly in the synthesis of methyl *tert*-butyl ether (MTBE) by etherification of isobutene with methanol [18].

Acidic ion-exchange resins of polystyrene-divinylbenzene (PS-DVB) are insoluble polymeric structures, long hydrocarbon chains structured by a cross-linking agent, with functional groups anchored that are capable to exchange ions with the medium and can be constructed from inorganic or organic monomer units. The most studied catalytic functional group is the sulfonic

acid. The acid form contains -SO_3H groups anchored in a polystyrene-based polymeric structure. These types of resins are common in some industrial processes and are intended to be used more widely in the future. If the medium is aqueous or strongly polar, the polymer chains separate, the resin beads swell and access to the -SO_3H groups is facilitated, producing a microenvironment in the resin pores similar to the liquid outside the resin.

1.2.3. Morphological structures

Acid ion exchange resins are produced in two basic morphological types: gel-type (microporous) and macroreticular (macroporous) resins. Both are spherical beads with a diameter in dry state usually in the range 0.3–1.2 mm. Both types can be conventional sulfonated when there is one sulfonic group per styrenic ring as a maximum or over sulfonated when there is more than one sulfonic group per styrenic ring [19].

Gel-type resins are rigid transparent beads and at microscopic scale its polymeric matrix is a homogeneous continuous structure. In the absence of water or strongly polar liquids, these may be ineffective in non-swelling media because the polymer chains do not practically separate and the inner part of the polymer matrix may be impermeable to reactive molecules, reducing the catalytic action to the few acidic groups remaining on the external surface of the resin beads. Therefore, catalysis by gel-type resins requires the use of a swelling medium capable of expanding the polymeric matrix. In swollen state, gel-type resins contain two types of pores: micropores for the inaccessible part of the matrix and new accessible mesopores formed on swelling which gradually disappear on shrinking [19].

Macroreticular resins are more widely used and are rigid opaque beads and present porosity independent of swelling of the polymer matrix. They are obtained by copolymerization of styrene and divinylbenzene in the presence of a solvent called 'porogen'. Macroreticular resins that are produced by suspension polymerisation, a pore forming agent is added. The concentration of the pore forming agent inside the droplets is low, so during particle growth the pore forming agent is included in the polymer phase. The size of the particles is in the millimetre range. After the polymerisation the pore forming agent is removed by evaporation or by solvent extraction. This creates the permanent porology of macroreticular resins. The concentration of the cross-linker inside the particles of commercial resins is uniform across the diameter because the polymer growth starts at many locations inside the whole droplet. The final particle is an agglomerate of many smaller particles as it can be seen in *Figure 5* [20].

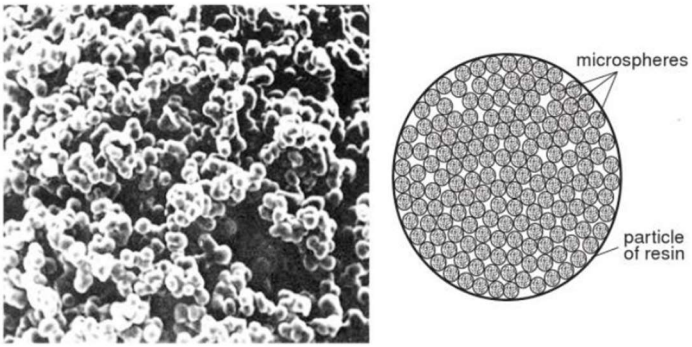

Figure 5. Illustration of a macroreticular resin. Scanning electron microscopy micrograph of macroporous resin Amberlyst-15 and its corresponding schematic representation. From [22].

The main features of macroreticular resins are their permanent pores with diameters in the range of 20-200 nm, their relative constancy of their shape and an opaque and rigid polymeric heterogeneous matrix structure [20]. They are composed of three types of pores: the micropores which are present in the inaccessible zone when the molecule is not embedded in the polymeric matrix, mesopores and macropores, conforming the permanent porosity. In a non-aqueous medium, they have a high porosity and surface area, to help maintain accessibility to acid groups.

Therefore, the catalytic activity of macroreticular resins is effective in both mediums, aqueous (strongly polar) and in nonaqueous (apolar). In a non-aqueous medium, they have a high porosity and surface area, to help maintain accessibility to acid groups. They are harder and more resistant due to the higher percentage of cross-linked with a larger surface area than gel-type. Despite these advantages, they can be fragile and because of their high degree of crosslinking internal mass transfer problems may be at play, involving lower activities due to the difficulty in reaching active sites and, they can have a lower thermal stability [19].

One of the properties discussed above is swelling degree. Resins undergo various morphological changes on swelling, by which spaces that did not exist in the dry state appear. Dried gel-type resins contain only micropores (spaces between the polymer chains). Mesopores appear when they swell in polar media (water,alcohol...), and disappear on shrinking in non-polar media as it can see in *Figure 6*. Macroreticular resins can be described as a collection of polymeric gel-phase microspheres interspersed by permanent pores. In a non-polar medium, these resins have macro and mesopores (between the aggregates of microspheres) and micropores (inside gel-type microspheres). Resins swelling generates an additional number of macro and mesopores, spaces that existed in the gel-phase in the range of micropores slightly increase their size, and at the same time, new spaces are formed within the gel phase [16].

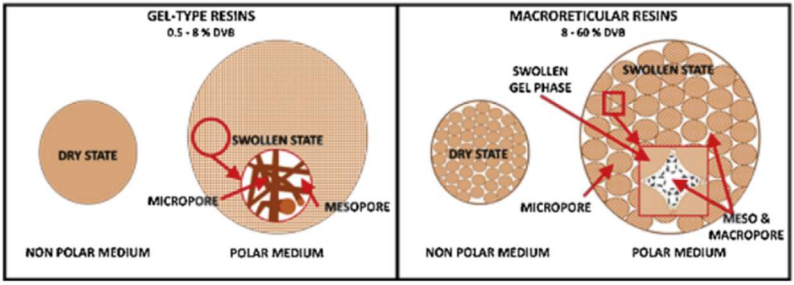

Figure 6. Morphological changes of gel-type and macroreticular resin particles due to swelling in polar media. [16]

2. OBJECTIVES

The main aim of the present project is to study the liquid-phase synthesis of mesityl oxide from acetone over a set of macroporous acidic ion-exchange resins. More specifically, the following subobjectives are set:

- To set up the experimental device and conditions to execute the experimental design proposed for the synthesis of mesityl oxide from acetone, including the analytical calibration of the system and the development of the analytical procedures.
- To identify and quantify the product distribution under the experimental conditions studied.
- To assess the conversion, selectivity and yield toward mesityl oxide of the resins evaluated.
- To determine the evolution of reaction rates during the course of the runs for the two main reactions involved in the two-step reaction in series.
- To elucidate the most relevant catalyst properties that favour the catalytic activity, conversion and selectivity toward the target product.
- To select an optimum catalyst for the synthesis of mesityl oxide over the range of acidic ion-exchange resins studied.

From this study, it will be possible to identify the optimum properties of the acidic resins for the targeted reaction, which can also be of utmost utility for the design of new bifunctional catalysts aimed at being used for the subsequent synthesis of MIBK by hydrogenation of mesityl oxide. Therefore, it will not only contribute to improve our knowledge on the reactions in-series studied, but it also can be a starting point for improving the industrial synthesis of MSO and MIBK.

3. EXPERIMENTAL

3.1. SETUP AND ANALYSIS

The experimental set up (*Figure 7*) consisted of the reactor, the thermostatic bath, and the analysis device. The reactor is an isothermal 200 mL stainless steel batch reactor (Autoclave Engineers Pennsylvania, USA) equipped with an overhead stirrer and heated with a jacket, in which the temperature is controlled using a thermostatic bath (Haake W13) at 90 ºC with a mixture of propanediol and water. With a thermocouple, with a precision of ±0,1 ºC, temperature inside the reactor can be measured. The pressure is kept constant at 3.0 MPa with N_2 to exceed the reaction mixture vapor pressure as well as to impel the samples to the analysis system. The stirring speed was set to 350 rpm approximately. The reactor is connected in-line to a GC (Agilent, 6890) equipped with a mass selective detector (MS, Agilent 5973N). The nitrogen gas, with a purity of 99.9995%, is used for the pressurization of the reaction at an overpressure of 3.0 MPa. The helium with a purity of 99.998% is used in the chromatographic analyses as a carrier gas.

The pressure inside the reactor was measured by a manometer and kept constant at 30 bar by injecting N2 (valve 6) from a pressurized cylinder into the reactor. A purging valve (V9) was used to reduce the reactor pressure when necessary for the recirculation of the sample after the analysis and before cleaning. The catalyst was injected using an injector by pressure difference (ca. 15 bar) and operating properly the valves V4,V3, and V2. N_2 was used to ensure the liquid phase of the reaction mixture by exceeding its vapor pressure at all conditions and to impel the sample towards the GC/MS.

The sampling was carried out periodically through the valve V7 that connects the reactor with the GC. In the sampling piping a 0.5 μm stainless steel filter was installed to prevent solids to reach the GC/MS. Once the sample had been taken and the GC analysis started, the remaining sample in the piping was recirculated by adequate operation of the valves V8 and V10

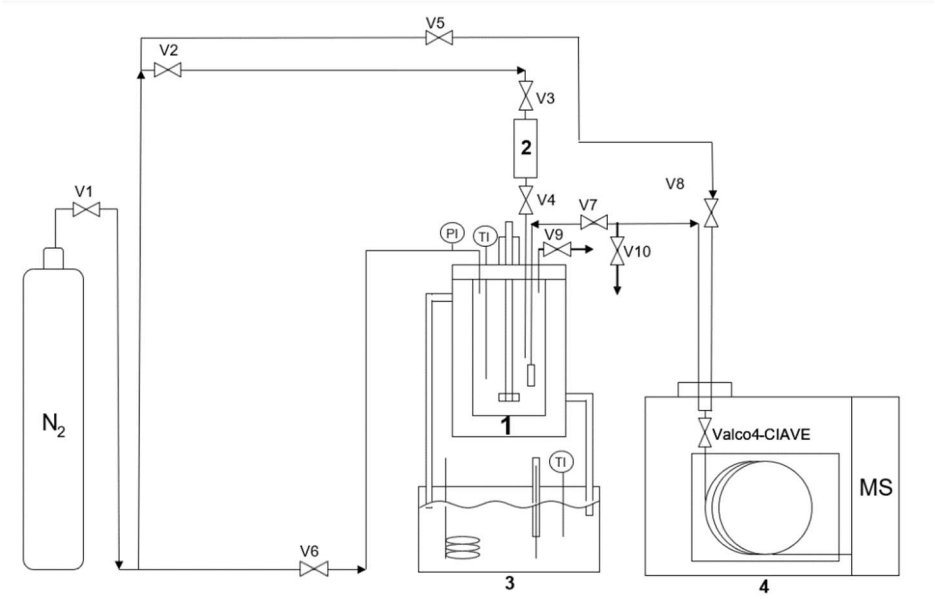

Figure 7. Experimental setup. 1: Batch reactor, 2: catalyst injector, 3: thermostatic bath, 4: gas chromatograph coupled to a mass selective detector.

3.1.1. Analytical methods

A gas chromatograph (7890B GC, Agilent Technologies Ltd.) coupled to a mass spectrometer selective detector (5977 GC/MSD, Agilent Technologies Ltd.) was used to analyze in situ the samples taken from the reactor. It is equipped with an injection valve, a carrier gas (He) supply, a capillary column (HP-PONA 19091S-001, J&W Scientific, Santa Clara, US; 100 % dimethylpolysiloxane, 50m × 0.20 mm × 0.50 µm), an oven, and the mass selective detector. In the analysis, 0.2 µL of the sample were injected into the GC/MS. The analytical procedure consisted of a constant temperature method that held 100 °C for 25 min, using a carrier gas flow of 1 mL/min, 2.515 bar and a split flow ratio 1000:1. The different compounds of the analyzed sample were eluted at different retention times in a chromatogram. By means of the calibration the different chromatographic areas were translated into mass for the quantification. Noteworthy, the detector allowed for the identification of the substances by comparing the mass spectra of

each individual compound eluted with the reference ones from the National Institute of Standards and Technology (NIST).

3.1.2. System calibration

To quantify the actual mass of each component, a calibration of the system was performed. Different standards of known amount in mass of each of the system components and in different relative proportions were prepared in glass vials, loaded into a pressurized burette (with N_2), and eventually injected through the GC/MS valve. The analyses for each standard were at least triplicated to ensure the reliability and reproducibility of the measurements. The measured chromatographic areas were then correlated with the known relative masses to obtain expressions able to quantify in terms of mass the analytical responses obtained during the catalytic activity tests. In all the cases, the calibration curves showed high correlation determination coefficients (R^2>0.99), reinforcing the reliability of the results. The corresponding plots are gathered in the *Appendix 1* and a summary of the calibration curves equations obtained is given in *Table 1*.

Table 1. Calibration equation for each component of the reaction

Compound	Calibration equation	R
Acetone	$W_{ac}=0.9856\cdot A_{ac}$	0.9999
MSO	$W_{MSO}=0.7998\cdot A_{MSO}$	0.9985
DAA	$W_{DAA}=1.5757\cdot A_{DAA}$	0.9848
i-MSO	$W_{i\text{-}MSO}=2.8598\cdot(A_{i\text{-}MSO})^2+2{,}3742\cdot A_{i\text{-}MSO}$	0.9883
Water	$W_{Water}= 19{,}654\cdot(A_{Water})^2+18{,}166\cdot A_{Water}$	0.9749

Where W_j is the mass fraction of each chemical species j and A_j is the area under the peaks expressed in unity basis.

3.2. CHEMICALS AND CATALYSTS

In all the experimental runs, the initial reactant is acetone with a purity of 99,5% (PanReac, Code: 131007.1211). In addition, the following reagents were used for the calibration of the system: mesityl oxide 99% mixture of alpha and beta isomers (93% MSO and 7%i-MSO) (Acros

organics, Code: 125600025), diacetone alcohol (Alfa Aesar, Code: 10231989), and deionized water.

The catalysts used in the activity tests were chosen based on their properties; a set of mainly macroreticular acid resins with a varied set of properties and one microporous resin. These are namely: Amberlyst™ 15 (A-15), Amberlyst™ 16 (A-16), Amberlyst™ 35 (A-35), Amberlyst™ 36 (A-36), Amberlyst™ 39 (A-39) Amberlyst™ 45 (A-45), Amberlyst™ 46 (A-46), Amberlyst™ 48 (A-48), Amberlyst™ DT (A-DT), Purolite® CT-175 (CT-175), Purolite® CT-275 (CT-275), and Purolite® MN-500 (MN-500). The only microporous resin tested was Purolite® CT124 (CT-124). A summary of relevant physicochemical properties for the selected catalysts can be seen in *Table 2*.

Table 2. Main physicochemical properties of the tested catalysts.

Catalyst	***Acid capacity[a]*** *[eq. H^+ kg^{-1}]*	***DVB[b] [%]***	***Max. operating T [°C]***	***Sulfonation type[c]***
A-15	4.81	20	120	C
A-16	4.80	15	130	C
A-35	5.32	20	150	O
A-36	5.4	20	150	O
A-39	4.81	8	130	C
A-45	3.65	Medium	170	S/Cl
A-46	0.87	High	120	S
A-48	5,62	High	140	O
A-DT	3.94	Medium	170	S/Cl
CT-175	4.98	High	145	C
CT-275	5.2	High	145	O
MN-500	2.70	Hyper	130	S
CT-124*	5.0	4	130	C

*The only microporous resin tested. [a]Titration against a standard base. [b]Crosslinking degree classification: low (7–12%); medium (12–17%); high (17–25%); hyper (>50%). [c]Conventionally sulfonated (C), oversulfonated (O), surface sulfonated (S) and sulfonated/chlorinated (S/Cl).

The morphological properties of resins vary depending on their swelling and likewise their structural properties determined by characterization. The main morphological properties obtained

from adsorption-desorption of N_2 in dry polymer state at 77 K by BET method, and those obtained in swollen polymer state by ISEC method are presented in *Table 3* [13].

Table 3. Morphological properties of IER evaluated in dry and swollen states [13].

Catalyst		Dry state polymer (BET)[b]				Swollen state polymer (ISEC)[g]				
	Skeletal density[a]	Surface area[c]	Pore volume[d]	Pore diameter[e]	Porosity[f]	"True pores"			Gel phase	
	ρ	Sg,BET	Vpore,BET	dpore,BET	θBET	Sg,ISEC	Vpore,ISEC	dpore,ISEC	Vsp[h]	θISEC[i]
	[g cm^{-3}]	[m^2 g^{-1}]	[cm^3 g^{-1}]	[nm]	[%]	[m^2 g^{-1}]	[cm^3 g^{-1}]	[nm]	[cm^3 g^{-1}]	[%]
A-15	1.416	42.0	0.33	31.2	31.7	156.9	0.63	16.1	0.77	49.5
A-16	1.401	1.7	0.01	30.8	1.8	149.3	0.38	10.3	1.13	52.8
A-35	1.542	34.0	0.21	24.7	24.5	198.9	0.72	14.5	0.61	51.3
A-36	1.567	21.0	0.14	27.2	18.3	146.5	0.33	9.1	1.03	53
A-39	1.417	0.1	$2.86 \cdot 10^{-4}$	12.7	0.0	56.0	0.16	11.1	1.62	60.3
A-40	1.431	0.2	$6.00 \cdot 10^{-4}$	10.9	0.1	11.0	0.13	45.5	0.44	–
A-45	1.466	49.0*	0.23	19.0*	25.4	220.2	0.52	9.5	0.97	54.4
A-46	1.137	57.4	0.26	18.3	23.0	186.0	0.48	10.3	0.52	12.3
A-48	1.538	33.8	0.25	29.5	27.7	186.0	0.57	12.3	0.62	45.3
A-DT	1.477	36.0*	0.20	22.0*	22.6	175.4	0.42	9.6	0.97	51.3
CT-124	1.420	0.1	$6.20 \cdot 10^{-4}$	35.7	0.1	0	0	0	1.90	62.9
CT-175	1.498	28.0	0.30	42.9	31.0	157.4	0.82	20.9	1.00	63.5
CT-275	1.506	20.3	0.38	74.4	36.2	209.4	0.77	14.7	0.81	57.9
CT-482	1.538	8.7	0.06	26.7	8.2	214.0	1.05	19.6	0.85	65.7
MN-500	1.539	332.0*	0.64*	152.0*	50.0	95.8	0.80	33.4	0.89	61.6

[a] Skeletal density. Measured by Helium displacement (Accupic 1330). [b] Samples dried at vacuum (10^{-4} mmHg, 110°C).[c] Brunauer-Emmett-Teller (BET) method. [d] Volume of N_2 adsorbed at relative pressure (P/P0)=0.99. [e] $d_{poreBET}=4V_{pore,BET}/S_{g,BET}$ or $d_{pore,ISEC}=4V_{pore,ISEC}/S_{g,ISEC}$. [f] $\theta_{BET}=V_{pore,BET}/V_{particle}=V_{pore,BET}/(V_{pore,BET}+1/\rho)$. [g] Measured with 0.2N aqueous solution of Na_2SO_4 as mobile phase except MN-500 where THF was used as mobile phase. [h] True volume of swollen polymer. [i] $\theta_{ISEC}=V_{pore,ISEC}/V_{particle}=(V_{pore,ISEC}+V_{sp}-1/\rho)/(V_{pore,ISEC}+V_{sp})$. *Manufacturer values.

Before being used in the activity tests, the catalysts were pre-treated to remove the initial moisture. First, approximately 3 g of the resin to be worked with is weighed out and left to dry for a few hours at room temperature. Finally, during the night in an oven at 383 K.

3.3. EXPERIMENTAL PROCEDURE

3.3.1. Swelling experiments

The degree of swelling of the different macroreticular resins used in the screening can be measured by means of the swelling ratio (SR), defined as the ratio of the volume of swollen resin, in a particular solvent or solvents mixture, to the volume of dry resin. Graduated glass cylinders of 50 mL were used in these measurements conducted at room conditions. 5mL of dry resin were weighed and loaded in the graduated test tube, which was subsequently filled with 30 mL of solvent. After 24h, SR was determined from the final volume of swollen polymer for each combination of resin and solvent.

3.3.2. Catalytic test experiments (screening)

The procedure for each catalytic activity experiment was essentially the same. From the density indicated by the supplier, (0,789 kg/L) 156.8 g, equivalent to 200 mL of acetone, were weighed. Subsequently, the reactor was filled with the correspondingly weighed amount of acetone, then it was sealed by tightening the screws. Later, the stirring (set to 750 rpm) and the thermostatic bath were switched on at the corresponding temperature, which in the case of the experiments carried out was always kept constant at 96 ± 2 ºC so that the reactor was maintained at 90 ± 2 ºC. Once the temperature inside the tank reached 90°C, the catalyst was injected. For all the experiments, a nominal mass of 1 g of resin was used.

The composition of the mixture in the reactor was sampled every 30 minutes for 7 hours by opening the valve connecting the reactor to the chromatograph. Impelled by N2, the sample is drawn into the valve connected to the column where, 0.2 µL of the sample is injected into the GC inlet carried by He. The analytical program of the GC consisted of a constant temperature 100 ºC period hold for 25 minutes.

The experimental conditions, e.g., mole of acetone and the corresponding catalyst for each experiment, are shown in *Table 4*.

Table 4. Experimental conditions of the catalytic activity tests.

Catalyst	Catalyst mass [g]	Initial acetone mole
A-15	1.002	2.74
A-16	1.013	2.70
A-35	1.009	2.72
A-36	1.004	2.70
A-39	1.005	2.74
A-45	1.015	2.69
A-46	1.008	2.70
A-48	1.020	2.71
A-DT	1.003	2.71
CT-175	1.009	2.73
CT-275	1.008	2.71
MN-500	0.839	2.71
CT-124	1.006	2.70

3.4. CALCULATIONS

The conversion of acetone (X_j), selectivity (S_j^k) and yield (Y_j^k) towards product *k* were calculated as follows for each sample:

$$X_j = \frac{\text{reacted mole of j}}{\text{initial mole of j}} \quad (1)$$

$$S_j^k = \frac{\text{produced mole of k}}{\text{reacted mole of j}} = \frac{n_k}{n_{MSO}+n_{DAA}+n_{i\text{-}MSO}} \quad (2)$$

$$Y_j^k = X_j \cdot S_j^k \quad (3)$$

j is referred to the reactant, acetone, and *k* is referred to the possible products; MSO, DAA or i-MSO.

The consumption rates of acetone and the formation rates of MSO at any instant were estimated from the derivative of the corresponding mole evolution curve by means of:

$$r_k = \frac{1}{W_{cat}}\left(\frac{dn_k}{dt}\right)_t \quad (4)$$

where r_k is the reaction rate of formation product *k* at time *t*, W_{cat} is the dry catalyst mass, and n_k is the mole of *k* formed. The mole evolution curve was fitted to empirical equations using *Curve Expert software* version 2.2.3. Initial reaction rates were calculated as the derivate of the mole evolution at the initial instant (t=0). The initial turnover frequency (TOF_i^0) of the catalysts expressed as [mol h^{-1} $eq.^{-1}$] were estimated as the ratio of r_k^0 to the acid capacity.

To validate the results, the mass balance in moles for each reaction sample must be fulfilled. Therefore, the percentage of compliance has been calculated with the following equation (5).

$$\%BM_{moles} = n_{ac,0} - n_{ac} - 2 \cdot n_{MO} - 2 \cdot n_{DAA} - 2 \cdot n_{i\text{-}MO} - n_{WATER} \quad (5)$$

The experimental error was evaluated by replicating the experiment with the resin CT-124. An average error between measurements of 2.6% for a 95% probability level, in mole basis, was obtained. With regards to the mass balance, it was fulfilled within ± 2.3% in all the runs. Therefore, the performed runs were considered reproducible and reliable.

4. RESULTS AND DISCUSSION

4.1. SWELLING EXPERIMENTS

It is well-known [17] that the resin morphology is affected by the chemical nature of the reaction medium, e.g. by swelling in polar media such as water, methanol and acetone. The dimenensionless solvatochromic solvent parameter normalized (EtN) is one of the most accurate used empirical scale to account for the solvent polarity effects [18]. It ranges from 0.000 (tetramethylsilane) to 1.000 (water). The EtN value for acetone is 0.355 whereas for mesityl oxide is 0.269, showing therefore a solvent polar nature. For comparison, the EtN values of methanol and ethanol are 0.762 and 0.701, respectively. Therefore, the resins are expected to undergo some shrinking across the course of the runs.

The volume of an IER grows when in contact with a liquid, particularly of polar nature, which affects the accessibility to active sites and hence, the catalytic activity of the ion exchangers is related to their swelling. In fact, there are many factors related to swelling, i.e., the resin crosslinking degree, the polar or non-polar nature of the solvent, the type of the functional group and their concentration. [21,22]. The SR was computed in the experiments using acetone. As shown *Figure 8*, the swelling experiments were carried out with macroreticular resins except for one, CT-124, the only gel-type resin tested. A-35, A-48 and CT-275 are oversulfonated resins. A-15, A-16, A-39 and CT-124 are conventionally sulfonated resins and A-46 and MN-500 are surface sulfonated resins [22].

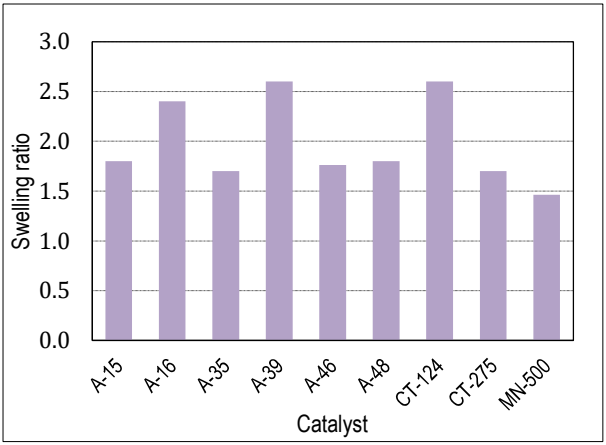

Figure 8. Swelling ratios obtained in acetone.

Resins with low %DVB swelled the most, with CT-124 being the resin with the highest swelling, followed by A-39. In contrast, the resin that swelled the least was MN-500 due to its high DVB content and, consequently, its rigid structure. As shown in previous studies [17], the expected swelling is inverse proportional to the crosslinking degree and so is the stiffness of the resin structure.

4.2. DESCRIPTION OF THE REACTION SYSTEM

The reaction system studied under the experimental conditions explored can be summarized by the pathway depicted in *Figure 2* to form MSO. The parallel formation of isomesityl oxide from diacetone alcohol in the last dehydration step is also to be considered.

Noteworthy, the formation of other byproducts such as those shown in Figure 3 was not detected in any of the runs conducted. Examples of the mole evolution for the distinct species is illustrated in *Figure 9* for two different resins used, exemplifying scenarios of low conversion (A-46) and high conversion (A-35).

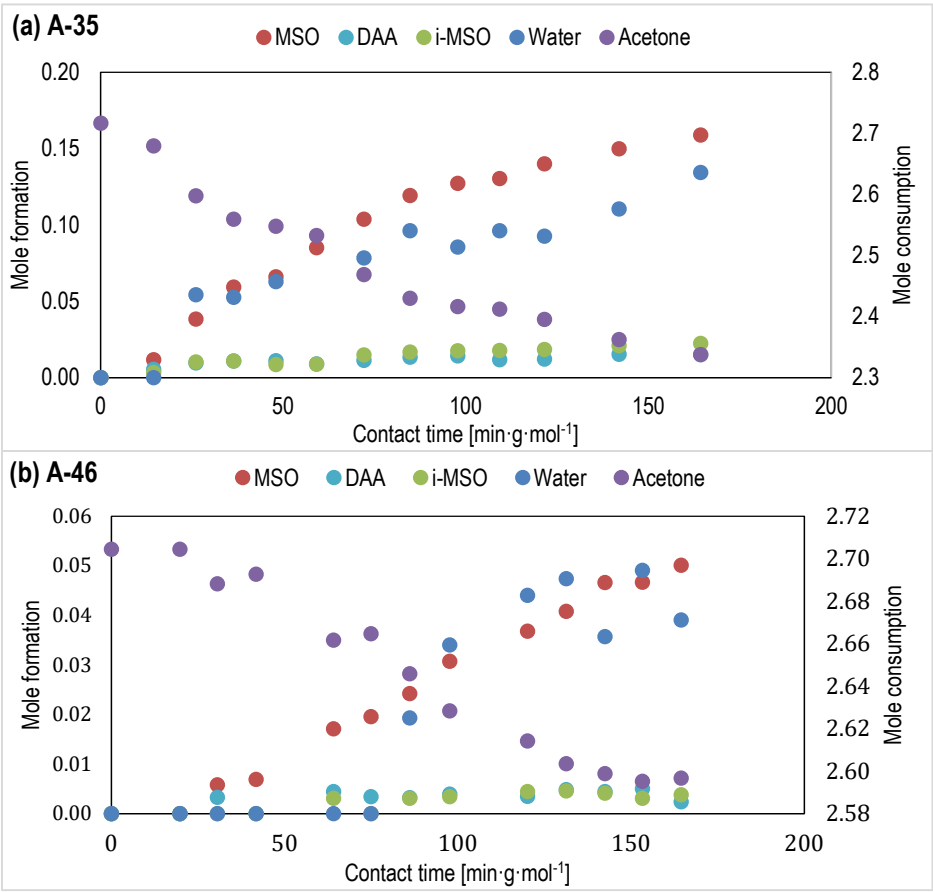

Figure 9. Mole evolution using A-35 (a) and A-46 (b) as catalyst. MSO, DAA, i-MSO and water mole formation (Left axis Y), and acetone consumption (Right axis Y)

All the experiments using different IER exhibited similar trends for the involved compounds. MSO was always the main product but DAA, i-MSO and water were also detected in increasing amounts over the course of the runs. The DAA mole detected at all instants for all resins indicates that, under the experimental conditions, DAA rapidly dehydrates to form MSO. The isomer of MSO is always formed in the reaction system, but in smaller quantities. Except for acetone, all the involved species showed a steadily increasing mole evolution with contact time, but with different increasing rate, as illustrated in *Figure 9*, depending on the catalyst used. It can then be concluded that it is very important to further study the properties of the catalyst that must justify the different generation rates of the desired product (MSO) obtained.

4.3. CONVERSION, SELECTIVITY AND YIELD

The acetone conversion evolutions obtained over the different resins studied vs. contact time are depicted in *Figure 10* for comparison. Although some overlapping exists, three patterns can be observed: i) Oversulfonated and conventionally sulfonated resins showed the highest acetone conversion, with a maximum of 14% for A-35, ii) sulfonated/chlorinated and those with medium crosslinking degrees reached medium conversions and finally, iii) surfaced sulfonated and gel-type resin presented the lower conversions with values less than 7%.

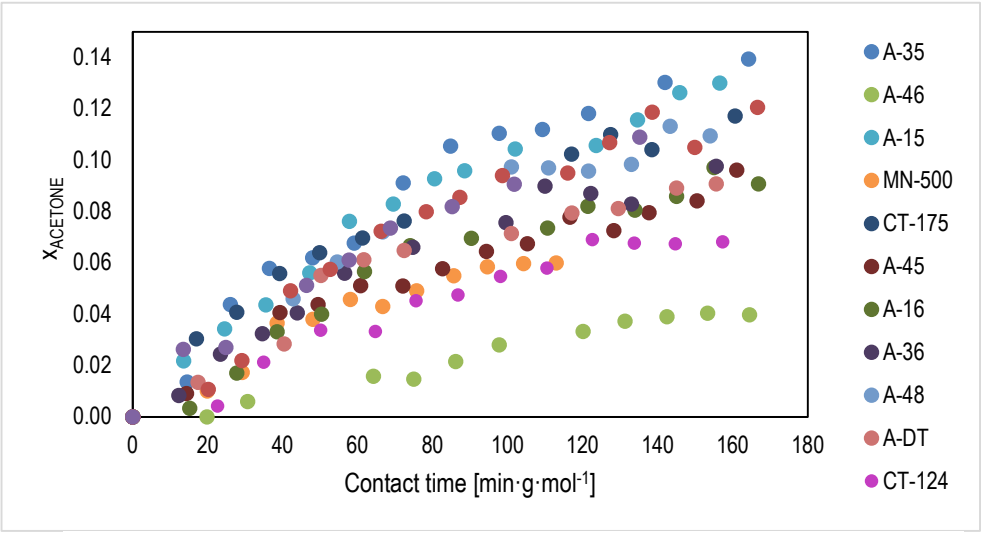

Figure 10. Acetone conversions obtained vs. its contact time for all IERs tested

Aiming to assess whether all the resins used are equally selective for obtaining the desired product, S_{Ac}^{MSO} of all IERs were compared versus acetone conversion. The fact that all resins tend to the same constant value, as shown in *Figure 11*, indicates that they are all equally selective to MSO at high conversion levels. The main differences are observed at low conversion and must be due do the different progress of each reaction in the initial steps of the runs.

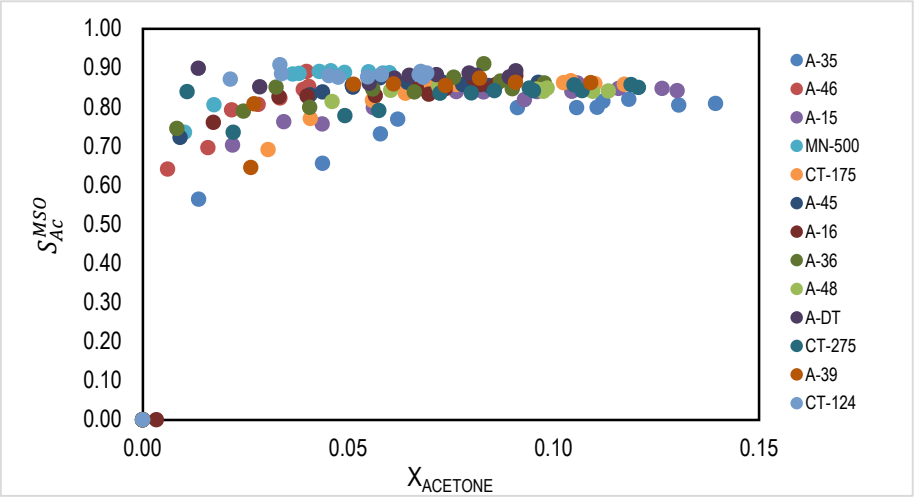

Figure 11. MSO selectivity vs acetone conversion for all the IERs

Figure 12 represents (S_{Ac}^{MSO}), (S_{Ac}^{DAA}) and (S_{Ac}^{i-MSO}) in the reaction studied vs contact time. Over all resins, MSO can be obtained as the main product under the experimental conditions since it was the most selective specie. The trend of its selectivity value over time in all analyses increased slightly in the early stages and finally was maintained constant at values around 85-86%. The low selectivity trend towards time in the DAA product, under the experimental conditions, was also similar in all the resins tested. Their initial values decreased slowly, and then remained at values of 4-5% by time. As can be seen in *Figure 12 (b),* at initial contact times the IERs A-35, A-39, A-46 and MN-500 presented higher selectivity as compared to the others. The formation of the corresponding MSO isomer showed constant selectivity by time to 9-10%, exposing a decrease in S_{Ac}^{k} of A-15, A-35, CT-175 and an increase in S_{Ac}^{k} of CT-124, MN-500 and A-DT at initial times.

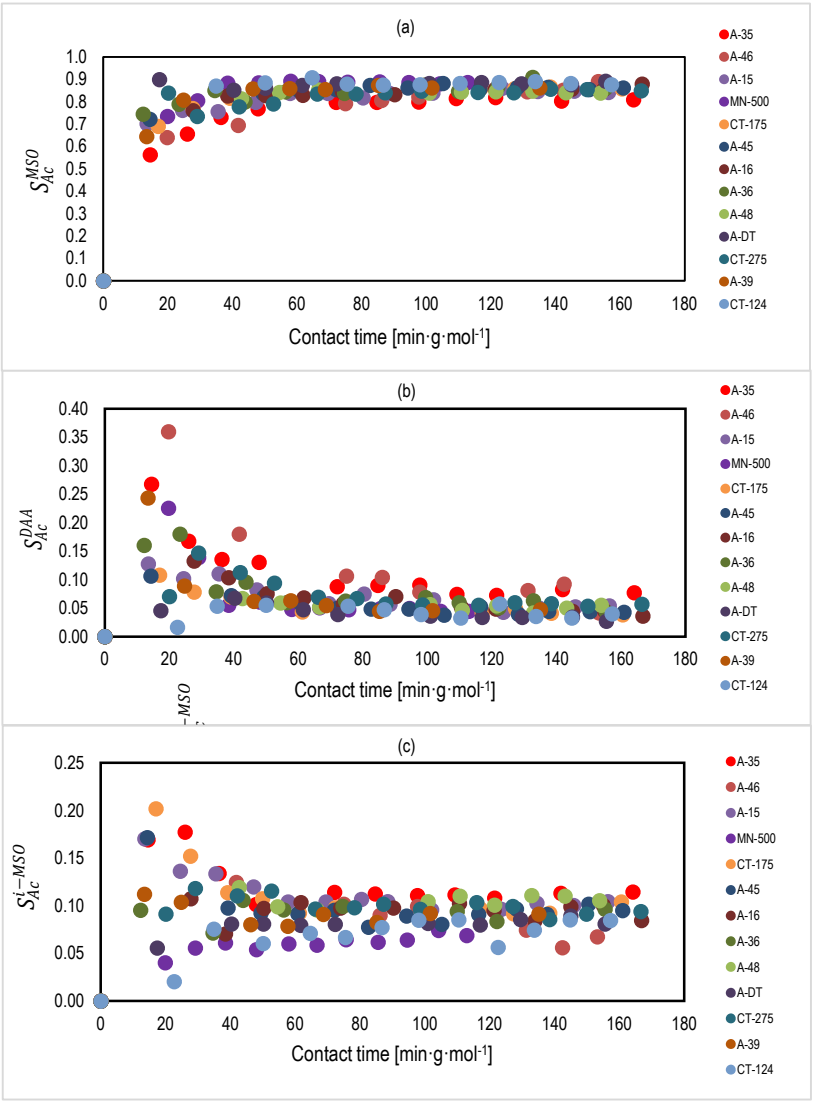

Figure 12. Selectivity of products towards time in all the IER tested. (a) S_{Ac}^{MSO} vs time (b) S_{Ac}^{DAA} vs time (c) S_{Ac}^{i-MSO} vs time

Examples of the yield evolution for different species is illustrated in *Figure 13* for two different resins, exemplifying scenarios of high conversion (A-35) and low conversion (A-46) in the analysed reaction. The acetone yield towards MSO increased almost linearly with contact time in both resins used. However, using A-35 resin, the yields obtained were notably higher, with a final value of approximately 11%, compared to the yields obtained with A-46 resin, which reached values below 4%. In contrast, the yields obtained for the rest of reaction products were virtually constant over time, not exceeding values of 2% and without significant differences between the catalysts with the highest and lowest activity.

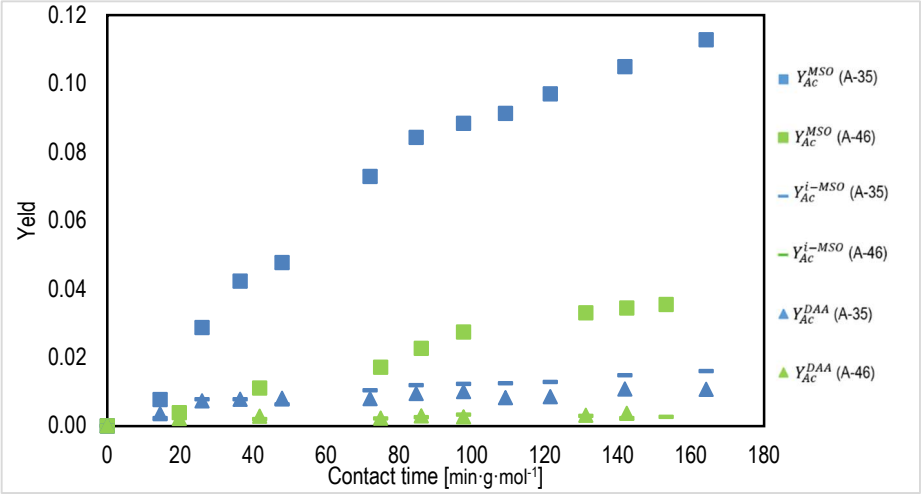

Figure 13. Yield of reactants towards product vs contact time using A-35 and A-45 as catalysts.

To appropriately compare the data for all IERs, *Table 5* shows a summary of the conversion, selectivity, and yield at contact time of approximately 160 [min·g·mol^{-1}].

Table 5. Conversion of acetone, selectivity and yield towards products of all catalysts tested.

Catalyst	$X_{Acetone}$ [%]	S_{Ac}^{MSO} [%]	S_{Ac}^{i-MSO} [%]	S_{Ac}^{DAA} [%]	Y_{Ac}^{MSO} [%]	Y_{Ac}^{i-MSO} [%]	Y_{Ac}^{DAA} [%]
A-15	13.01	84.17	10.45	5.39	10.95	1.36	0.70
A-16	9.08	87.96	8.47	3.57	7.99	0.77	0.32
A-35	13.95	80.87	11.46	7.67	11.28	1.60	1.07
A-36	9.77	86.11	9.62	4.27	8.42	0.94	0.42
A-39	10.91	86.17	9.13	4.70	9.33	1.03	0.55
A-45	9.63	86.22	9.49	4.28	8.30	0.91	0.41
A-46	3.98	89.08	6.75	4.17	3.55	0.27	0.70
A-48	10.95	83.95	10.56	5.50	9.19	1.16	0.60
A-DT	9.08	89.21	8.09	2.70	8.10	0.74	0.25
CT-175	11.73	85.77	10.42	3.81	10.06	1.22	0.45
CT-275	12.07	84.93	9.39	5.68	10.23	1.13	0.71
MN-500	6.01	88.70	6.89	4.41	5.33	0.41	0.26
CT-124	6.83	87.61	8.45	3.95	5.98	0.58	0.27

The results illustrated in the *Table 5* indicate that catalysts with higher acid capacity provide higher acetone conversion and yield of the desired product (MSO). Note however that the gel-type resin CT-124, although characterized by high acid capacity, presented comparable results to the low performing macroreticular catalysts. This result might be caused by the absence of permanent pores which leads to a reduction of the actives centres efficiency. The less active catalyst for obtaining MSO was A-46. A remarkable property of this resin is the small amount of sulphonic groups within the gel-phase since sulphonation is limited to the first few layers of styrene rings [19]. it can be assured that the presence of sulphonic groups located in the gel-phase clearly promotes the formation of MSO.

4.4. **CATALYTIC ACTIVITY RELATION WITH MORPHOLOGICAL PROPERTIES**

Initial formation rates of MSO were calculated as mentioned in section 3.4. Other studies of the reaction system [10], shown that the dehydration step of DAA to form MSO is enhanced in acidic media. For this reason, the formation rates over time of a resin with high acid capacity (A-35), intermediate acid capacity (A-45) and low acid capacity (A-46) had been compared in *Figure 14*. The largest experimental initial formation rates were obtained over the resin with the

highest acid capacity A-35. In resins with such an acid capacity, the acid site distribution in the catalyst particle is nearly homogeneous [17]. In all the cases and as expected, the MSO formation rate trend decreased with time, being the exponential-like decrease more pronounced for the resins that showed higher initial activity. The low acid capacity resin A-46 showed a low constant almost linear trend over time. For resins with lower acid capacity, sulfonation is restricted to the outer layers since sulfonation proceeds from the external to the internal layers of the particle [17] and this fact, in contrast with resins with higher acid capacity, presented disadvantages for the present reaction.

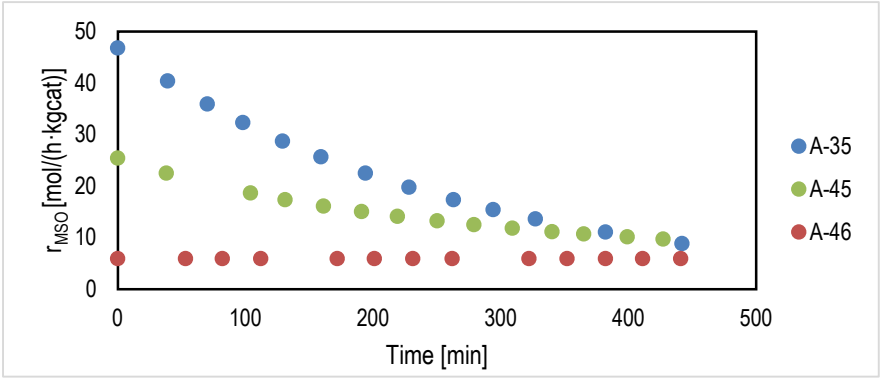

Figure 14. Velocity of MSO formation over time in A-35, A-45 and A-46.

Table 6 summarizes the initial MSO formation rates and $\mathrm{TOF}^{0}_{\mathrm{MSO}}$. TOF is used to give a numerical quantification of the number of molecules reacted per active sites of catalyst. As seen in *Table 6*, A-35 was the most active resin in the MSO formation. In contrast, A-46 was the least active resin. It is relevant to highlight that TOF numbers over these resins obtained are considerably low if compared to other systems, e.g. etherification of olefins with alcohols [20].

Table 6. Initial formation of MSO rates and TOF^0_{MSO} for the IER tested.

Catalyst	r^0_{MSO} [mol/(h·kgcat)]	TOF^0_{MSO} $[mol/(h \cdot eq)]$
A-15	32.96	6.85
A-16	29.18	6.08
A-35	46.79	8.80
A-36	32.19	5.96
A-39	38.73	8.05
A-45	25.44	6.97
A-46	5.95	6.84
A-48	39.38	7.01
A-DT	33.52	8.51
CT-124	17.97	3.59
CT-175	38.46	7.72
CT-275	32.94	6.33
MN-500	25.21	9.34

Globally, oversulfonated and conventionally sulfonated macroreticular IER (A-35, A-48, A-39, CT-175) with high acid capacity yielded the fastest r^0_{MSO} confirming that the second step of the reaction studied is favoured by acidic media. For this reason, the catalysts with lower acidic capacities A-45, A-46 and MN-500 presented the lowest ratios comparable to the ratio obtained by the only gel-type resin CT-124. It is noteworthy that the gel-type catalyst CT-124 showed a low TOF^0_{MSO} value despite having an acidic capacity similar to those of A-39 and CT-175 macroreticular resins. Thus, the absence of permanent pores influences the relative efficiency of the active sites which can be associate to accessibility limitations detrimentally. This indicates that the main role of macropores is to provide spaces that facilitate the accessibility to the actives sites located within the inner part of the polymer, which increases the relative efficiency of active sites (TOF^0_{MSO}). In the interest of clearly relate which attributes of the resins favor the formation of MSO, their initial formation times were related to their properties in *Figure 15.*

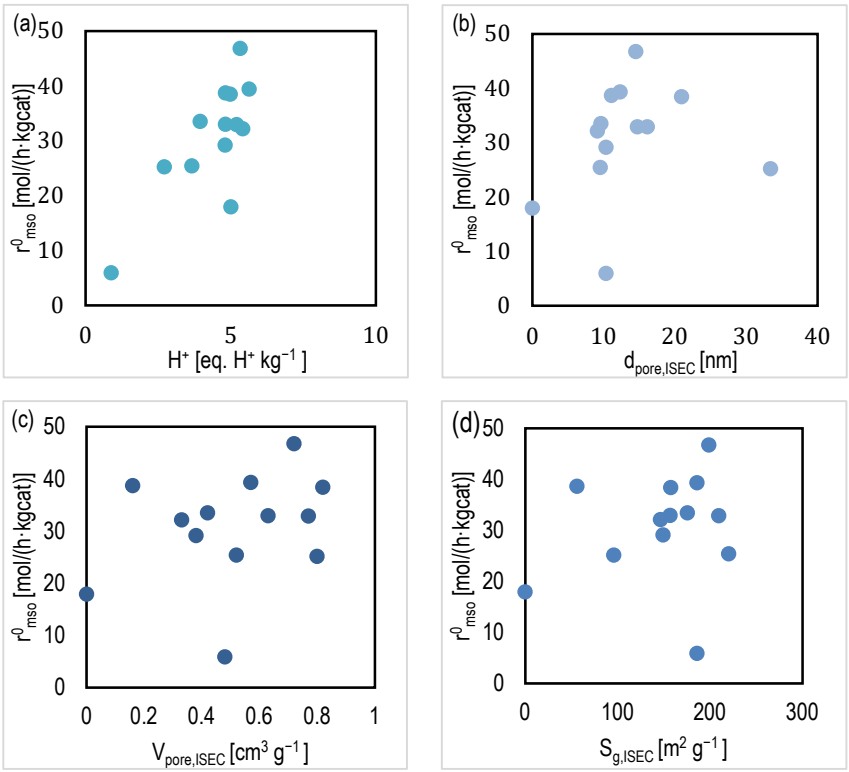

Figure 15. Initial velocity rates of the different catalyst compared with their acid capacity (a), macropore diameter (b), macropore volume (c) and macropore surface (d).

Clearly, resins with high acid capacity, as shown in *Figure 15 (a)*, showed better results, which can somewhat be also observed for the pore diameter (Figure 15 b); generally the catalytic activity increased with $d_{pore,ISEC}$ values. On the other hand, no clear relationship are inferred from *Figure 15 (c)* and *(d)*, the case of macropore volume and macropore surface area, as it was the case for the relations with catalysts properties determined in dry-state, not represented for simplicity.

The use of morphological properties determined by ISEC should be, in principle, more adequate to establish relations with catalytic activity and to represent the actual catalysts working state in the present reaction system than those properties determined in dry state. This agrees and is further reinforced by the swelling experiments performed, in which the SR ratio obtained in

acetone, was comparable to those determined in water and ethanol for similar resins [17]. As mentioned above, the degree of swelling depends on the interaction of the catalyst with the solvent and on the degree of crosslinking. The distinctive parameter of this model is the specific volume of the swollen polymer (V_{sp}), defined as the volume of free space plus the skeleton volume. In *Figure 16* this parameter was compared with initial reaction rates for all the catalysts. The overall trend for resins with higher initial rates was relatively low V_{sp} values, except for the case of the resin A-46 (the lowest activity reported). As mentioned above, low values of swollen polymer volume result in low swelling capacity.

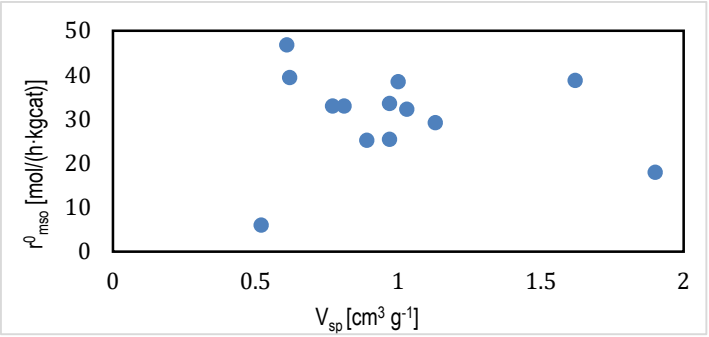

Figure 16. initial velocity ratios of each catalyst compared with specific volume of swollen polymer in water

The high catalytic activity obtained for the resins with high acid capacity (e.g., A-35) and their generally low values of the volume of the swollen polymer indicate that the catalytic activity of IERs might be related to the ratio $[H^+]/V_{sp}$. The plotting of r^0_{MSO} values vs. $[H^+]/V_{sp}$ (see *Figure 17*) shows a steadily increasing trend exhibiting a close to linear relationship, which thus indicates that high acid capacities and low V_{sp} values are desired features for the present system to

maximize the production of target product (MO). The linear fit was computed giving a value of R^2=0,93.

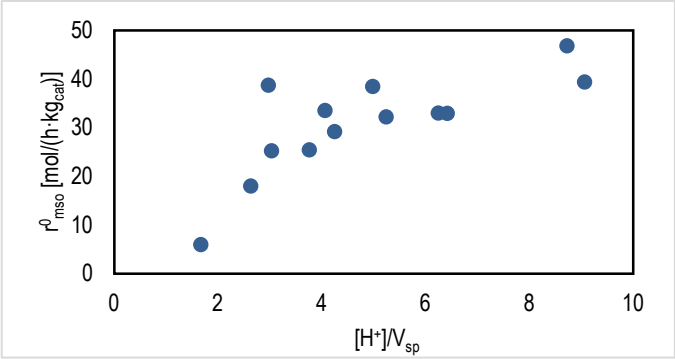

Figure 17. r^0_{MSO} vs ratio of acid capacity to volume of the swollen polymer.

Therefore, since the acid capacity depends on the sulfonation degree of the polymer, IER with high concentration of sulfonic groups and with low volume of swollen polymer are the best option for the formation of MSO. A high concentration of sulfonic groups in a reduced space can allow cluster formation or coordination of active sites. Furthermore, this result also brings the deduction that the crosslinking degree and macropores play a determinant role, since they make the permeation of molecules easier promoting the accessibility to active sites.

The polymer density zone distributions of the swollen gel phase obtained by ISEC for the tested IERs are shown in *Figure 18*. Differences in the structure of the polymer skeleton, including the location of sulfonic groups in the catalyst matrix, explain the differences between the level of activity of each resin and even the different active sites within its structure. The microporous structure of ion-exchange resins is modeled as a set of discrete volume fractions with different characteristic polymer chain densities as it can be seen in *Figure X* [20]. It can be observed that denser polymer fractions are higher in macroreticular resins. Also, the resistance of MN-500 to swelling consequence of its extremely high crosslinking degree (50%) is reflected in its low polymer fraction volume. Finally, larger contributions of the densest polymer zone to the total gel-phase volume of the swollen polymer were visible in conventionally sulfonated resins (CT175 and

A-15) as compared to their respective oversulfonated versions (CT-275 and A-35). Nevertheless, the opposite trend was detected in A-16 and A-36.

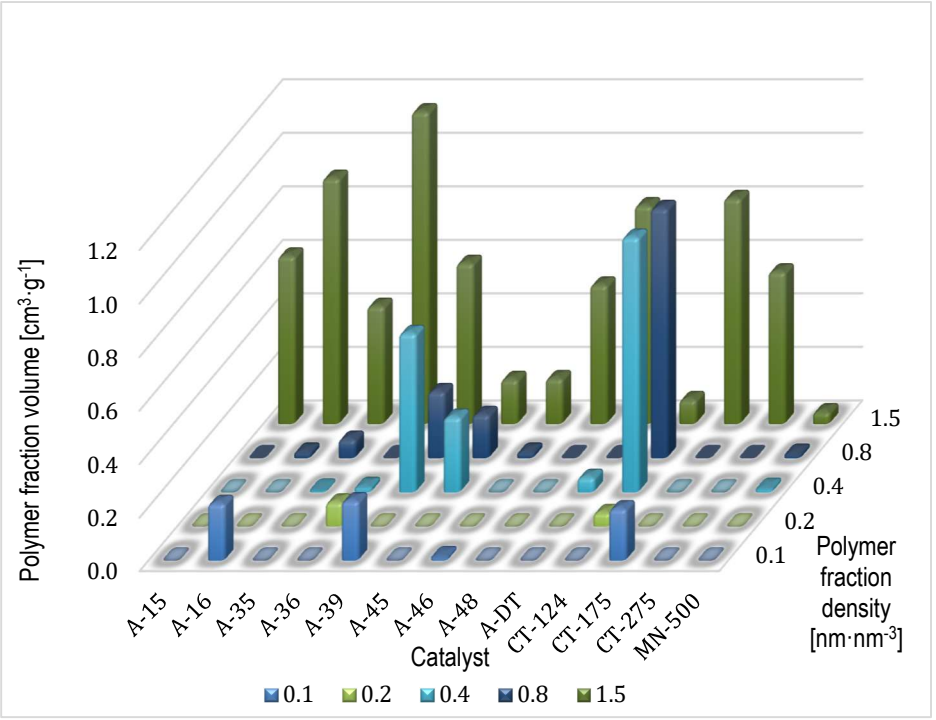

Figure 18. Characterization of the polymer fractions of the assayed catalysts.

In the present reaction, a maximum of specific activity was shown in the zone of highest polymer density (1.5 nm/nm^3), due to the large number of active sites. Therefore, it can be argued that resin domains of higher polymer chain density are presumably those that enhance the observed catalytic activity.

5. CONCLUSIONS

The main objective of this work was to relate the catalysts morphological properties with the activity for the liquid-phase synthesis of mesityl oxide from acetone over a set of macroporous acidic ion-exchange resins. This has been successfully achieved by coducting experimental catalytic activity tests from where the following conclusions are extracted:

All resins were found to be active for obtaining mesityl oxide. In addition to the desired product, diacetone alcohol, iso-mesityl oxide and water were also obtained. Relatively low conversions of acetone were obtained in all the runs, which perhaps can be improved by increasing the catalyst loads and/or the runs duration. The acetone selectivity values towards MSO were notably high (85-90%). In addition to the differences in terms of conversion and selectivity, different catalytic activity in terms of mesityl oxide formation rates are also observed, which are linked to the different structural and physicochemical properties of the catalysts.

After assessing the relations of catalytic activity with dry and swollen state morphological properties of the studied resins, a correlation between initial MSO formation rates and $[H^+]/V_{sp}$ is observed; both increase with each other proportionally and following a close to linear trend. This explains the highest activity reported for the resins A-35 and A-48 and are reinforced by the swelling ratio experiments conducted that indicate that the polar nature of the reaction medium promotes the swelling of the catalysts. Finally, it can be stated that the resins domains of highest density of polymer chain are presumably those boosting the catalytic activity observed, which along with the $[H^+]/V_{sp}$ relation found can be explained by the favorable formation of clusters of active sites.

.

REFERENCES AND NOTES

[1] "Disolvente - Wikipedia, la enciclopedia libre." https://es.wikipedia.org/wiki/Disolvente (accessed May 18, 2022).

[2] J. H. Clark, T. J. Farmer, A. J. Hunt, and J. Sherwood, "Opportunities for bio-based solvents created as petrochemical and fuel products transition towards renewable resources," *Int. J. Mol. Sci.*, vol. 16, no. 8, pp. 17101–17159, Jul. 2015, doi: 10.3390/IJMS160817101.

[3] "Acetone - The Chemical Company." https://thechemco.com/chemical/acetone/ (accessed May 21, 2022).

[4] F. E. Liew *et al.*, "Carbon-negative production of acetone and isopropanol by gas fermentation at industrial pilot scale," *Nat. Biotechnol. 2022 403*, vol. 40, no. 3, pp. 335–344, Feb. 2022, doi: 10.1038/s41587-021-01195-w.

[5] "European Solvents Industry Group - ESIG - ESIG European Solvents Industry Group." https://www.esig.org/ (accessed May 18, 2022).

[6] C. de Prada Alumna and I. Lessa Victoria Henao, "'Modelado matemático y simulación para mejorar la producción de butanol en la fermentación ABE,'" 2013.

[7] W. K. O'Keefe, F. T. T. Ng, and G. L. Rempel, "Experimental studies on the syntheses of mesityl oxide and methyl isobutyl ketone via catalytic distillation," *Ind. Eng. Chem. Res.*, vol. 46, no. 3, pp. 716–725, Jan. 2007, doi: 10.1021/IE060812P.

[8] F. Liguori, C. Oldani, L. Capozzoli, N. Calisi, and P. Barbaro, "Liquid-phase synthesis of methyl isobutyl ketone over bifunctional heterogeneous catalysts comprising cross-linked perfluorinated sulfonic acid Aquivion polymers and supported Pd nanoparticles," *Appl. Catal. A Gen.*, vol. 610, p. 117957, Jan. 2021, doi: 10.1016/J.APCATA.2020.117957.

[9] Lizbeth Alejandra Mar Magaña, "Síntesis y caracterización del catalizador MgO/CaO para una reacción de condensación aldólica", *Esc. Super. Ing. química e Ind. Extr.*, vol. Síntesis y, 2008.

[10] M. Marczewski, Y. Kavalchuk, U. Ulkowska, M. Gliński, and O. Osawaru, "Diacetone alcohol decomposition and benzaldehyde Cannizzaro reaction as test reactions for the basic strength measurements of alumina, magnesia, Amberlyst type resins (A-15, XN 1010, A-26, A-21), Nafion NR 50 and solid sulfuric acid", doi: 10.1007/s11144-018-1492-z.

[11] S. Talwalkar and S. Mahajani, "Synthesis of methyl isobutyl ketone from acetone over metal-doped ion exchange resin catalyst," *Appl. Catal. A Gen.*, vol. 302, no. 1, pp. 140–148, Mar. 2006, doi: 10.1016/J.APCATA.2006.01.004.

[12] W. Nicol and E. L. Du Toit, “One-step methyl isobutyl ketone synthesis from acetone and hydrogen using Amberlyst® CH28,” *Chem. Eng. Process. Process Intensif.*, vol. 43, no. 12, pp. 1539–1545, Dec. 2004, doi: 10.1016/J.CEP.2004.02.008.

[13] R. Soto López, “Simultaneous etherification of C 4 and C 5 iso-olefins with ethanol over acidic ion-exchange resins for greener fuels”, doi: 10.1016/j.cherd.2013.11.012.

[14] C. Izquierdo, J. F., Cunill, F., Ejero, J., Iborra, M., & Fité, “Cinética de las reacciones químicas,” Edicions Universitat Barcelona, 2004, p. (1st ed., pp. 143–268).

[15] E. Van De Steene, J. De Clercq, and J. W. Thybaut, “Kinetic Study of Acetic Acid Esterification with Methanol Catalyzed by Gel and Macroporous Resins,” vol. 25, no. 4, 2014.

[16] E. Ramírez, R. Bringué, C. Fité, M. Iborra, J. Tejero, and F. Cunill, “Assessment of ion exchange resins as catalysts for the direct transformation of fructose into butyl levulinate,” *Appl. Catal. A Gen.*, vol. 612, Feb. 2021, doi: 10.1016/J.APCATA.2021.117988.

[17] R. Soto, C. Fité, E. Ramírez, M. Iborra, and J. Tejero, “Catalytic activity dependence on morphological properties of acidic ion-exchange resins for the simultaneous ETBE and TAEE liquid-phase synthesis,” *Cite this React. Chem. Eng*, vol. 3, p. 195, 2018, doi: 10.1039/c7re00177k.

[18] C. Reichardt and T. Welton, “Solvents and Solvent Effects in Organic Chemistry: Fourth Edition,” *Solvents Solvent Eff. Org. Chem. Fourth Ed.*, Nov. 2010, doi: 10.1002/9783527632220.

[19] J. Guilera, E. Ramírez, C. Fité, J. Tejero, and F. Cunill, “Synthesis of ethyl hexyl ether over acidic ion-exchange resins for cleaner diesel fuel,” *J. Name*, vol. 00, pp. 1–3, 2013, doi: 10.1039/x0xx00000x.

[20] C. Fité Piquer Roger Bringué Tomàs, “Synthesis of ethers as oxygenated additives for the gasoline pool Jordi Hug Badia i Córcoles”.

[21] F. Liguori, C. Oldani, L. Capozzoli, N. Calisi, and P. Barbaro, “Liquid-phase synthesis of methyl isobutyl ketone over bifunctional heterogeneous catalysts comprising cross-linked perfluorinated sulfonic acid Aquivion polymers and supported Pd nanoparticles,” 2020, doi: 10.1016/j.apcata.2020.117957.

[22] “Ion Exchange Materials: Properties and Applications - Andrei A. Zagorodni - Google Llibres.” https://books.google.es/books?hl=ca&lr=&id=XfDFKl3I74MC&oi=fnd&pg=PP1&dq=ion+exchange+resin+application&ots=AP-IbHcnwB&sig=WC-bmfIRMrmsY7zx9r9Ay46oh9k#v=onepage&q=ion exchange resin application&f=false (accessed Jun. 04, 2022).

ACRONYMS

MIBK	Methyl isobutyl ketone
MSO	Mesityl oxide
DAA	Diacetone alcohol
IER	Ion-exchange resins
PS-DVB	Polystyrene-divinylbenze
DVB	Divinylbenze
GC	Gas chromatogram
MS	Mass selective detector
W_j	Mass fraction
A_j	Area under the peak
A-15	Amberlyst™ 15
A-16	Amberlyst™ 16
A-35	Amberlyst™ 35
A-36	Amberlyst™ 36
A-39	Amberlyst™ 39
A-45	Amberlyst™ 45
A-46	Amberlyst™ 46
A-48	Amberlyst™ 48
A-DT	Amberlyst™ DT
CT-175	Purolite® CT-175
CT-275	Purolite® CT-275
MN-500	Purolite® MN-500
CT-124	Purolite® CT-124

SR	Swelling ratio
Vsp	Volume of the swollen polymer
TOF_i^0	Initial turnover frequency
EtN	Solvatochromic solvent parameter normalized

APPENDICES

APPENDIX 1: SYSTEM CALIBRATION PLOTS

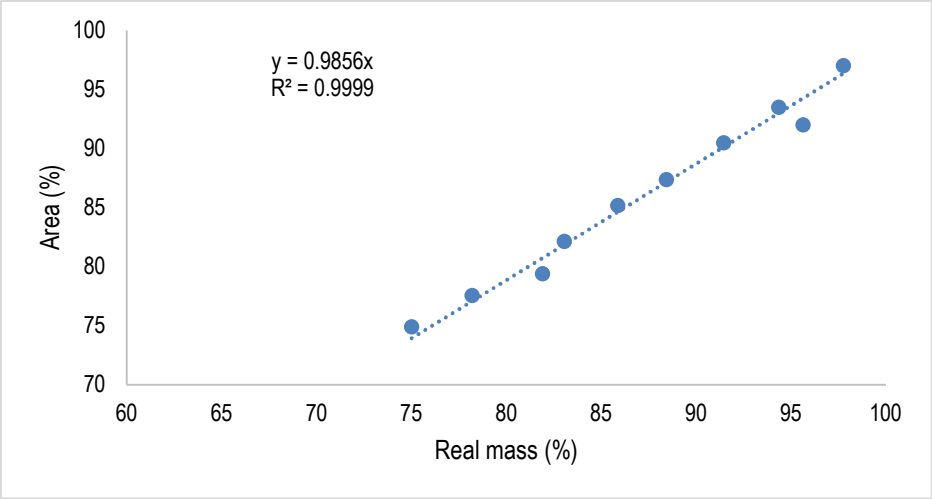

Figure 19. Calibration plot - acetone

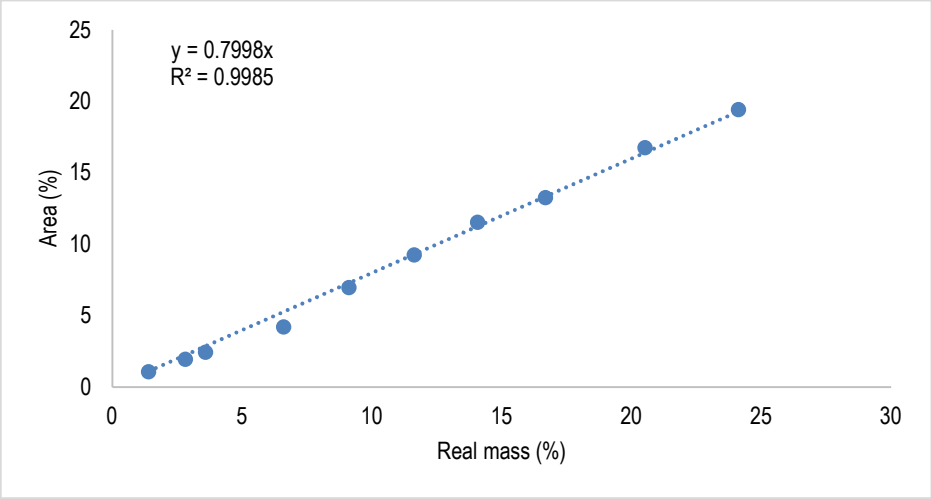

Figure 20. Calibration plot - MSO

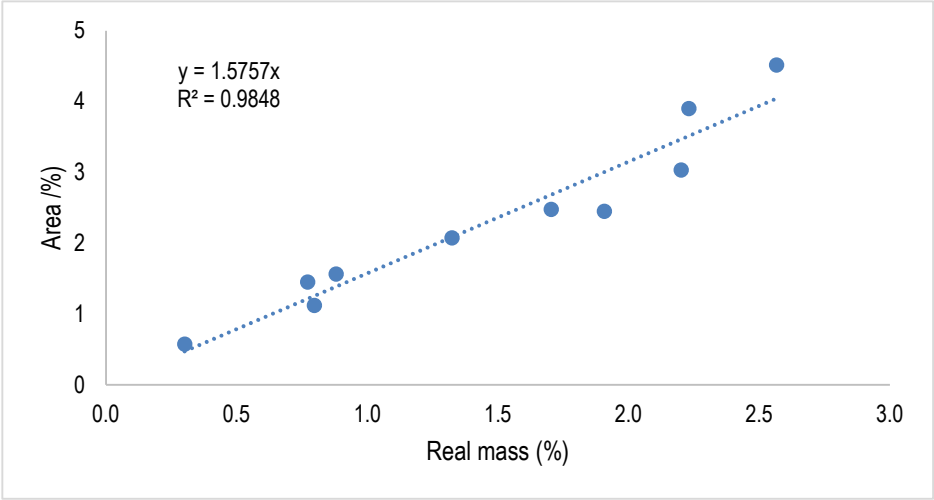

Figure 21. Calibration plot - DAA

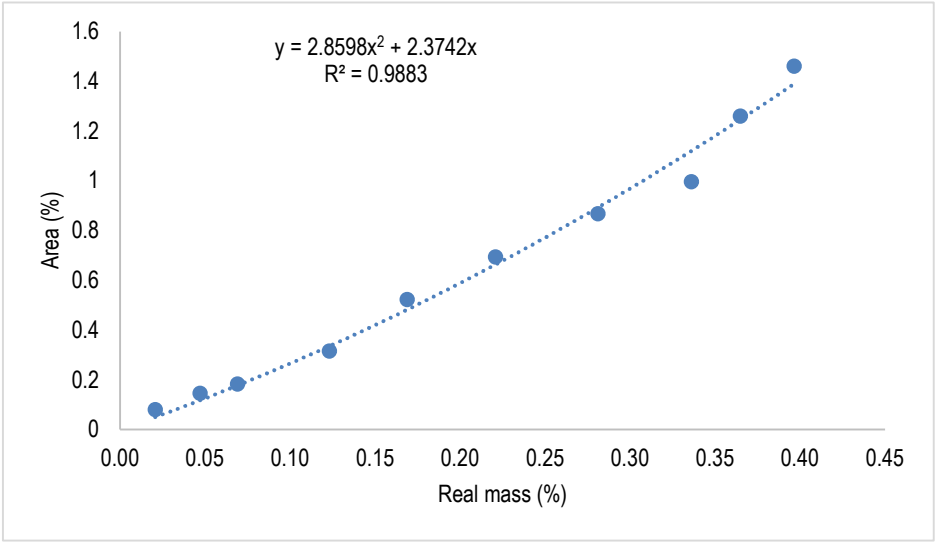

Figure 22. Calibration plot – i-MO

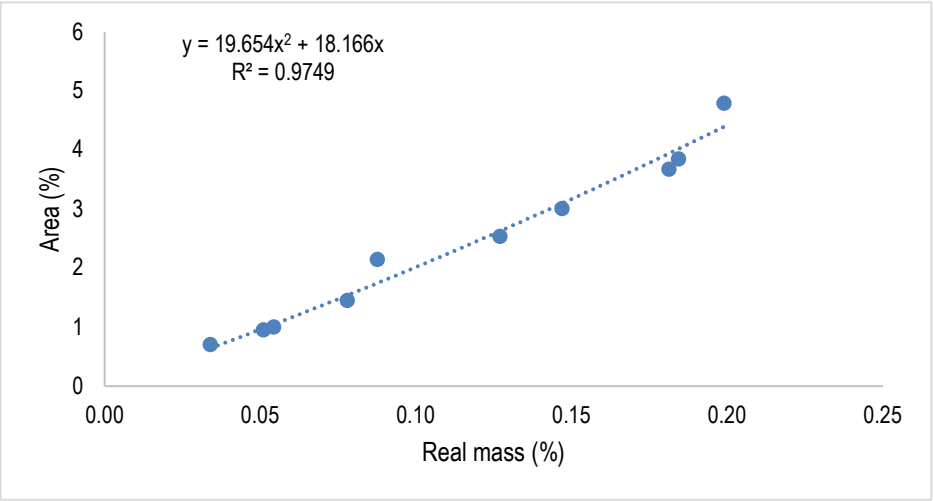

Figure23. Calibration plot - water